

Magnetocapacitance: Probe of Spin-Dependent Potentials

K. T. McCarthy and A. F. Hebard*

Department of Physics, University of Florida, Gainesville, Florida 32611-8440

S. B. Arnason

Department of Physics, University of Massachusetts, Boston, Massachusetts 02125

(Received 9 July 2002; published 17 March 2003)

The magnetic field dependence of the capacitance of Pd-AlO_x-Al thin-film structures has been measured. The observed quadratic dependence of capacitance on the magnetic field is consistent with a theoretical model that includes the effect of a spin-dependent electrochemical potential on electron screening in the paramagnetic Pd. This spin-dependent electrochemical potential is related to the Zeeman splitting of the narrow *d* bands in Pd. The quantitative details depend on the electronic band structure at the surface of Pd.

DOI: 10.1103/PhysRevLett.90.117201

PACS numbers: 75.50.Pp, 72.25.Dc

The design and implementation of spintronic devices demands accurate experimental characterization of magnetic metals and semiconductors. Specifically, a detailed understanding of metal-semiconductor and metal-dielectric interfaces is necessary. Three examples illustrate this point: efficient spin injection from a ferromagnetic metal into a semiconductor depends critically on interface properties [1,2]; the spin polarization of the tunneling current in magnetic tunnel junctions is affected by spin-dependent surface screening in the ferromagnetic electrodes [3]; and the magnitude of the magnetoresistance in giant magnetoresistance is determined in part by the quality of the interfaces between ferromagnetic and nonmagnetic layers [4]. The study of these and other interface effects facilitates a better understanding of the relevant physics in these devices.

This project is motivated by Zhang's theoretical work [3] involving electron screening in ferromagnets. According to Zhang, both Coulomb and exchange interactions influence the screening response. This fact is represented theoretically by a spin-dependent potential decaying exponentially into the surface of a ferromagnet in the presence of an electric field applied perpendicular to the surface. The spin dependence originates from the exchange splitting of spin-up and spin-down bands. In this Letter, we present the magnetic field dependence of the screening length λ of paramagnetic Pd which arises from a magnetic field-induced spin splitting of the density states. This spin dependence of the screening potential in Pd is captured in magnetocapacitance measurements. Our technique demonstrates a static probe of magnetic field-induced spin-dependent potentials involving a voltage and no current. This is in contrast to previous work [1,2,4,5] involving current-driven spin accumulation.

When a capacitor is fabricated with a thin-film spacer layer, a significant portion of the potential drop can occur across the metal-insulator interfaces [6,7]. This is shown schematically in the inset in Fig. 1. The applied voltage V , the dielectric constant κ , the dielectric thickness d , and

the screening length λ determine the magnitude of these interfacial voltage drops. The measured capacitance of a thin metal-insulating-metal structure is thus indicative of bulk dielectric as well as interfacial properties that include dependence on λ [6,8–10]. The variation of screening length with magnetic field results in a magnetic field-dependent capacitance. We chose Pd as our model system because of its large Pauli paramagnetic susceptibility. We measured the magnetic field-dependent capacitance (magnetocapacitance) of Pd-AlO_x-Al thin-film structures and determined that the screening length of Pd increases quadratically with applied magnetic field.

Our structures are grown and characterized in the following way. First we use dc-magnetron sputtering to

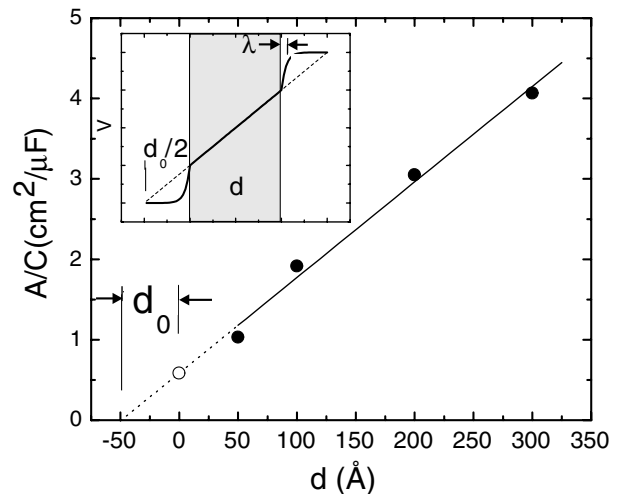


FIG. 1. Inverse areal capacitance versus dielectric thickness for four Pd-AlO_x(*d*)-Al structures at 10 K. The negative of the *x* intercept gives the additional effective thickness d_0 , which is 49 Å from a linear fit. Similarly, the inverse slope determines that the permittivity κ of our AlO_x is 9.5. The inset illustrates our model of potential versus position in which two metallic electrodes are separated by a dielectric (shaded region) of thickness d . The screening length is given by λ .

deposit 1000 Å of Pd onto the entire surface of a square silicon substrate (1 cm²). A calibrated thickness of AlO_x is then grown over the entire Pd surface via reactive ion beam sputter deposition of Al in an oxygen ambient at a carefully controlled pressure. This technique has been shown [10] to produce dense, high quality, amorphous AlO_x. The final deposition step utilizes a shadow mask with 1 mm diameter circular holes placed in close proximity to the sample through which Al is thermally grown.

The sample is inserted into a Quantum Design QD6000 cryostat in a custom sample probe with coaxial electrical leads attached to the sample. The bottom of the sample probe is an electrically isolated shielded enclosure that houses the sample. Three terminal capacitance measurements are made using an AH-2700 capacitance bridge. All measurements are performed in an electrically screened room. Capacitance was measured at a frequency of 1 kHz and at temperatures and magnetic fields ranging from 300 to 10 K and -7 to 7 T, respectively.

Figure 1 shows the inverse areal capacitance versus dielectric thickness at 10 K for four Pd-AlO_x-Al structures with dielectric thickness ranging from 50 to 300 Å. The linear dependence of inverse capacitance on thickness with nonzero intercept implies that the geometrical capacitance C_g is in series with a thickness independent interface capacitance C_i determined largely by the screening lengths in the two electrodes. Other contributions to C_i , such as interface states and surface roughness, are present. These additional contributions give rise to enhanced dispersion at low frequency [8]. By plotting inverse capacitance versus dielectric thickness, we are able to infer the magnitude of the interface capacitance C_i and an effective length scale d_0 , which defines the crossover plate separation below (above) which C_i (C_g) dominates. C_i is equal to the reciprocal of the y intercept (open circle) and d_0 is the x intercept. As d approaches zero (and C_g diverges), the measured capacitance C_m approaches C_i . Our simple model for the capacitance of our structures is shown schematically in the inset in Fig. 1 where the electrostatic potential, which decays exponentially into each electrode, is plotted versus position. For such a structure, C_m is given by

$$\frac{A}{C_m} = \frac{A}{C_i} + \frac{A}{C_g} = \frac{d}{\kappa\epsilon_0} + \frac{d_0}{\kappa\epsilon_0}, \quad (1)$$

where $d_0 = \kappa(\lambda_1 + \lambda_2)$. The area is given by A , λ_1 and λ_2 are the screening lengths in the metallic electrodes, and ϵ_0 is the permittivity of free space. This model accurately accounts for our observed thickness dependence. It also shows us how capacitance measurements are sensitive to the screening lengths in the electrodes of capacitors having sufficiently thin spacer layers ($d \approx d_0$).

We observe that the capacitance of our structures decreases quadratically with magnetic field (indicating a quadratic increase in λ) as shown in Fig. 2. In this plot, the normalized change in capacitance versus H^2 is linear

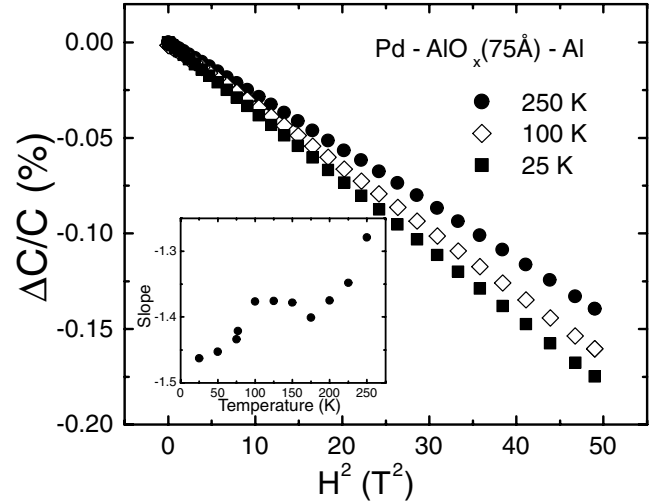


FIG. 2. Plot of $100(C(H) - C(0))/C(0)$ versus H^2 for Pd-AlO_x(75 Å)-Al at the three temperatures shown in the legend. The slopes of these curves are plotted versus temperature in the inset.

with a negative slope. The weak temperature dependence of the slope is shown in the inset. Strain effects can be ignored since the linear magnetostriction in Pd films is zero to within one part in 10⁶ [11].

By observing negative magnetocapacitance, we are explicitly inferring the H dependence of the screening length of Pd since λ is the dominant field-dependent quantity, as discussed later in this Letter. The H dependence comes from the field-induced spin splitting of the conduction band of Pd. Using a Stoner model of electron-electron interactions, the spin-dependent energy of an electron is given by

$$\epsilon^{\uparrow,\downarrow} = \epsilon(\mathbf{k}) + U_0 n^{\uparrow,\downarrow} \mp \mu_B H - e\phi(x), \quad (2)$$

where U_0 is the energy that determines the strength of the interactions, $\epsilon(\mathbf{k})$ is the band energy, μ is the chemical potential, $\phi(x)$ is the electrostatic potential, e is the magnitude of the charge of the electron, μ_B is the Bohr magneton, and the spin-up (-down) carriers are determined by the minus (plus) sign preceding the Zeeman energy ($\mu_B H$). Further, the spin-dependent carrier concentration at the surface of a metal with an electric field applied normally (at $T = 0$) is given by

$$n^{\uparrow,\downarrow}(x) = \frac{1}{2} \int_0^{\mu - U_0 n^{\uparrow,\downarrow} \pm \mu_B H + e\phi(x)} N(\epsilon) d\epsilon, \quad (3)$$

where $N(\epsilon)$ is the density of electronic states. If we expand the density of states around the Fermi level, keep only the lowest order terms in H and $\phi(x)$, and require charge conservation in the absence of an electric field (to find the H dependence of the chemical potential μ), we find that the total carrier concentration a distance x into the surface of the metal is given by

$$n^l(x) + n^r(x) = n_0 + N(\epsilon_F) \left(\frac{1}{1+J} \right) \left[1 + \frac{1}{2} \left(\frac{1}{1+J} \right) \left(\eta + \frac{2J}{1-J} \left[\frac{N'}{N} \right]_{\epsilon_F}^2 \right) \left(\frac{\mu_B H}{1-J} \right)^2 \right] e\phi(x), \quad (4)$$

with

$$\eta = \left[\frac{N''}{N} - \left(\frac{N'}{N} \right)^2 \right]_{\epsilon_F} \quad (5)$$

and $J = \frac{1}{2} U_0 N(\epsilon_F)$. Poisson's equation must be satisfied self-consistently, yielding an exponentially decaying solution for the electrostatic potential over a length scale (screening length) given by

$$\frac{1}{\lambda^2} = \frac{1}{\lambda_{TF}^2} \left(\frac{1}{1+J} \right) \left[1 + \frac{1}{2} \left(\frac{1}{1+J} \right) \left(\eta + \frac{2J}{1-J} \left[\frac{N'}{N} \right]_{\epsilon_F}^2 \right) \times \left(\frac{\mu_B H}{1-J} \right)^2 \right], \quad (6)$$

where $\lambda_{TF}^{-2} = e^2 N(\epsilon_F) / \epsilon_0$. All state densities and derivatives are evaluated at the Fermi energy ϵ_F . We note that the temperature and magnetic field dependence of the magnetic susceptibility of Pd are treated similarly in the literature [12–14]. In fact, η is the same band parameter that determines the strength of the temperature dependence of the magnetic susceptibility of Pd at low temperatures, namely:

$$\chi_T = \chi_0 \left[1 + \frac{\pi^2}{6} \eta D (k_B T)^2 \right], \quad (7)$$

where $\chi_0 = \mu_B^2 D N(\epsilon_F)$ and $D = 1/(1-J)$ is the Stoner enhancement factor [12]. The Stoner-enhanced Pauli paramagnetic susceptibility is given by χ_0 and we have neglected terms of order T^4 and higher.

We digress a moment to discuss the validity of the $T = 0$ assumption in the above derivation. One might expect thermal broadening to smear out the magnetic field dependence of λ . Including temperature in the calculation of the carrier concentration by way of the Sommerfeld expansion introduces, to lowest nontrivial order in T , two additional terms to Eq. (6), both of which are quadratic in T . One of these terms is independent of field; the other is quadratic in both T and H . This quartic term can be neglected since the perturbations due to temperature and field are both very small compared to the Fermi energy. Thus, temperature and field are uncoupled to lowest nontrivial order. This argument applies equally well to the temperature dependence of the magnetic susceptibility in Pauli paramagnetism [Eq. (7)], in which case the spin splitting occurs at the Fermi energy as well. Since the magnetic moment is not thermally smeared appreciably, one would not expect smearing to wash out the field dependence in the screening case.

The capacitance of a structure containing one electrode with a magnetic field-dependent screening length as given by Eq. (6) (to quadratic order in H) is

$$\frac{C(H) - C(0)}{C(0)} = \frac{C(0)}{A} \left[\frac{\lambda_{TF}}{4\epsilon_0} \left(\frac{1}{1+J} \right)^{3/2} \gamma \left(\frac{\mu_B H}{1-J} \right)^2 \right], \quad (8)$$

where

$$\gamma = \eta + \left(\frac{2J}{1-J} \right) \left[\frac{N'}{N} \right]_{\epsilon_F}^2. \quad (9)$$

Consolidating all of the H dependence into the Pd electrode is justified by our observation that magnetocapacitive effects in Al-AlO_x-Al structures are at least an order of magnitude smaller than the same in Pd-AlO_x-Al structures. This observation, coupled with our expectation that the roughness in both types of junctions is similar, suggests that surface roughness alone is not contributing significantly to the magnetocapacitance. Furthermore, the capacitance exhibits very little frequency dependence below 250 K, indicating that the majority of interface states are inactive and hence also do not contribute.

Assuming that the screening lengths of Al and Pd are similar, and using the values of d_0 and κ determined from Fig. 1 (49 Å and 9.5, respectively), we estimate the $H = 0$ screening length of Pd, $\lambda_{TF}/(1+J)^{1/2}$, to be ≈ 2.5 Å. This length is artificially large since it attributes all of the interface capacitance C_i to the screening response of the electrodes, thereby neglecting surface roughness and interface states [8], which contribute very little to the field dependence, as mentioned above. Using the ($H = 0$) screening length, the slope of the $\Delta C/C$ vs H^2 curve, and Eq. (8), we estimate the strength of the field dependence γ to range from -100 to -1000 eV⁻². This value varies from sample to sample, indicating the sensitivity of the magnetocapacitance effect to interface quality. Andersen [12] performed a bulk calculation of η for Pd using a rigid band approximation. He reported a value of 12 eV⁻², but it should be noted that the screening length of a metal depends on its surface band structure, which may differ substantially from the bulk band structure. Equation (9) implies that there is also an additional term that contributes to the strength of the magnetic field dependence of the screening length, which is absent in the temperature dependence of the magnetic susceptibility ($\gamma > \eta$). The presence of exchange interactions simply renormalizes the Zeeman energy in the case of the susceptibility, as shown in Eq. (7) ($D \approx 10$) [12].

The chemical potential μ in Pd lies so close to an inflection point in the density of states versus energy that any perturbation resulting in a small change in μ can affect the magnitude and sign of η . We believe the chemical potential in the Pd electrode near the Pd-AlO_x interface lies very near a peak in the density of states,

which accounts for our observation that $\gamma < 0$ (therefore, $\eta < 0$) as determined by magnetocapacitance measurements. Indeed, it is predicted that doping Pd with additional d electrons (e.g., alloying with Ag), thereby modifying the chemical potential, causes the sign of η to reverse [12]. The sign change in η arises from a competition between the first and second derivatives of the state densities at the Fermi level as indicated in Eq. (5).

The capacitance of our structures is temperature dependent and decreases linearly (at high temperatures) with decreasing temperature, as shown in Fig. 3. The inset shows a capacitance (normalized to 10 K) versus temperature for three AlO_x thicknesses and indicates a trend toward stronger temperature dependence for thicker oxides. The first correction to the Thomas-Fermi screening length due to temperature is quadratic; therefore, the operative mechanism behind the temperature dependence is not electronic in nature except, perhaps, at the lowest temperatures. We attribute the temperature dependence in the linear regime to temperature-dependent strain in the metallic electrodes in conjunction with a temperature-dependent dielectric constant, which accounts for our observation of stronger temperature dependence for thicker oxides: as the oxide thickness is increased, the capacitance is more strongly dependent upon bulk dielectric properties.

Other effects may contribute, such as the freezing out of electron traps at the interfaces and reduced frequency dispersion as the temperature is lowered. The negative magnetocapacitance becomes larger in magnitude as the capacitance decreases (Fig. 2, inset; y axis contains only negative values). This is curious as the magnetocapacitance should scale as shown in Eq. (8) with the $H = 0$ capacitance $C(0)$. Though we do not fully understand this dependence, one possible contribution to this phenom-

non is as follows: since the freezing out of traps in the interface removes a subset of localized charged levels, a larger fraction of the net interfacial charge resides in the electrodes themselves, and thus a larger potential drop is associated with electric field penetration into the electrodes. Only the induced charge within the Pd electrode contributes to the magnetocapacitance; therefore, we expect the magnetic field dependence to be stronger when, at lower temperatures, a larger portion of the potential drop occurs due to electric field penetration into the Pd electrode. In addition, the magnetic susceptibility of palladium shows a very strong dependence on temperature with a pronounced peak near 80 K [14]. As indicated in Eq. (7), the origin of this peak depends on the same band structure factor η that appears in our magnetocapacitance calculations. Accordingly, it is not surprising that we observe a similar extremum in the slope of the $\Delta C/C$ vs H^2 curve (Fig. 2, inset).

In conclusion, we have measured the magnetic field dependence of the screening length of paramagnetic Pd via magnetocapacitance. We have proposed a model that captures the essence of the relevant physics of this effect. We have also shown that magnetocapacitance measurements reveal surface band structure, which is distinct from bulk band structure. Since magnetocapacitance is sensitive to spin-dependent electrochemical potentials, it may be a technique capable of measuring nonequilibrium spin polarization in spin-injection devices. Novel, low carrier density materials, e.g., dilute magnetic semiconductors, may show similar magnetocapacitive effects larger in magnitude due to longer screening lengths.

The authors acknowledge useful discussions with Dmitrii Maslov and Pradeep Kumar. This work was supported by NSF DMR-0101856.

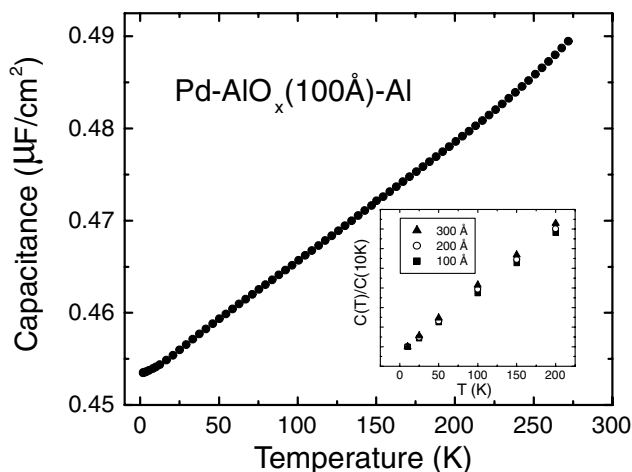


FIG. 3. Plot of areal capacitance versus temperature for Pd- $\text{AlO}_x(100 \text{ \AA})$ -Al. The inset shows normalized capacitance versus temperature for structures with AlO_x thicknesses indicated in inset legend.

*Electronic address: afh@phys.ufl.edu

- [1] P. Hammar, B. Bennett, M. Yang, and M. Johnson, Phys. Rev. Lett. **83**, 203 (1999).
- [2] D. Smith and R. Silver, Phys. Rev. B **64**, 045323 (2001).
- [3] S. Zhang, Phys. Rev. Lett. **83**, 640 (1999).
- [4] J. Ben Youssef, K. Bouziane, O. Koshkina, H. Le Gall, M. El Harfaoui, M. El Yamani, J. Desvignes, and A. Fert, J. Magn. Magn. Mater. **165**, 288 (1997).
- [5] M. Johnson, Phys. Rev. Lett. **70**, 2142 (1993).
- [6] C. A. Mead, Phys. Rev. Lett. **6**, 545 (1961).
- [7] J. G. Simmons, Appl. Phys. Lett. **6**, 54 (1965).
- [8] K. McCarthy, S. Arnason, and A. Hebard, Appl. Phys. Lett. **74**, 302 (1999).
- [9] J. Krupski, Phys. Status Solidi B **157**, 199 (1990).
- [10] A. Hebard, S. Ajuria, and R. Eick, Appl. Phys. Lett. **51**, 1349 (1987).
- [11] J. Schmidt and L. Berger, J. Appl. Phys. **55**, 1073 (1984).
- [12] O. Andersen, Phys. Rev. B **2**, 883 (1970).
- [13] M. Beal-Monod and J. Lawrence, Phys. Rev. B **21**, 5400 (1980).
- [14] S. Misawa, Phys. Rev. Lett. **26**, 1632 (1971).